Curved Rays Anisotropic Tomography: Local and Global Approaches

Zvi Koren, Igor Ravve, Paradigm and Dan Kosloff, Tel-Aviv University and Paradigm*

Summary

Curved Rays Tomography updates background anisotropy velocity parameters in the time-migrated domain. The tomography uses image gathers generated by Anisotropy Curved Rays Kirchhoff Time Migration. A locally varying 1D Vertical Transverse Isotropy (VTI) model is assumed. The background anisotropy parameters are the instantaneous (interval) vertical compression velocity V and the two Thomsen anisotropy parameters δ and ε. Interval velocity (or alternatively δ) is updated from short offsets reflection events, while ε is updated from the available long offset data. Two complementary approaches are presented in this study: local and global. In the local approach, the medium parameters are updated from top down, layer by layer, one parameter at a time. The residual anisotropy parameters, that best fit the residual moveout curves, are picked. The residual moveout includes overburden and current layer components. In the global approach, all parameters are inverted simultaneously. Due to a large number of offsets, the problem becomes over-defined, and we solve it by a constrained least-squares minimization. The cost function accounts for data and model variances, which reflect the reliability of the data and control parameter variations, respectively. The updated parameters are constrained to a feasible range.

VTI Parameters and their Range

The VTI medium is described by five Thomsen (1986) parameters, but to study the compression waves, four parameters suffice. Furthermore, the ratio between the vertical compression and shear velocity is commonly assumed constant, $f = V^2/V_S^2 = 1/4$. Three parameters remain: the vertical compression velocity V and the two Thomsen anisotropy parameters, δ and ε. The limits for δ depend on the ratio f, $\delta^{\min} = -(1-f)/2 = -3/8$, $\delta^{\max} = 2f/(1-f) = 2/3$ (Tsvankin, 2001). In practice we keep this range narrower, $-0.2 \le \delta \le 0.5$. The second Thomsen parameter ε is theoretically limited only from below. Since the Poisson ratio is positive, $\varepsilon > -1/4$. Laboratory and field data indicate that the velocity in the isotropy plane (horizontal velocity) is usually larger than the vertical velocity V. This means that ε is positive, and we accept the range $0 \le \varepsilon \le 0.5$. The range of the anellipticity $\eta \equiv (\varepsilon - \delta)/(1+2\delta)$ is defined as $-0.05 \le \eta \le 0.2$ and leads to an additional constraint.

Initial and Boundary Value Anisotropic Ray Tracing

Ray tracing is a core element of seismic tomography. In a 1D medium the horizontal slowness of the ray is constant. We distinguish between *initial value* ray tracing (IVRT) and *boundary value* ray tracing (BVRT). IVRT considers a single ray with a given horizontal slowness and vertical time at the starting point. The goal of BVRT is to find the parameters of a specific ray pair (incident and reflected). We assume both rays emerge from the image point and arrive to the surface. The vertical time and the orientation of the reflection surface are specified at the reflection point, and the offset length and azimuth refer to the earth surface.

Initial Value Ray Tracing

In a 1D model, the initial value ray tracing is two-dimensional. The ray path is a curved line within a single vertical plane. Let h be horizontal coordinate in this plane. The vertical coordinate is depth z or vertical time t_o. Tracing is done numerically by solving a set of ordinary differential equations. The governing function is the Hamiltonian, which depends on two components of slowness: horizontal, $p_h = \text{const}$, and vertical, p_z, and on the properties of the medium, which in turn, depend only on vertical time t_o. The Hamiltonian function follows from the Christoffel equation for P-SV waves,

$$G(p_h, p_z, z) = \frac{K - L \cdot V^2 - V^{-2}}{2 \cdot (1-f)} \quad , \qquad (1)$$

where parameters K and L are

$$K = (1+f)\cdot\left(p_h^2 + p_z^2\right) + 2\varepsilon\, p_h^2$$
$$L = f\left(p_h^2 + p_z^2\right)^2 + 2\varepsilon\, p_h^2\left(f p_h^2 + p_z^2\right) - 2\delta(1-f)\, p_h^2\, p_z^2 \qquad (2)$$

The Hamiltonian vanishes at any point along the ray. The resolving ray tracing equations are

$$\frac{dh}{d\sigma} = \frac{\partial G}{\partial p_h} \; , \quad \frac{dz}{d\sigma} = \frac{\partial G}{\partial p_z} \; , \quad \frac{dp_z}{d\sigma} = -\frac{\partial G}{\partial z} = -\frac{1}{V}\cdot\frac{\partial G}{\partial t_o} \; , \qquad (3)$$

where σ is an independent integration parameter. The traveltime along the ray can be computed using

$$\frac{dt}{d\sigma} = \frac{\partial t}{\partial h}\cdot\frac{dh}{d\sigma} + \frac{\partial t}{\partial z}\cdot\frac{dz}{d\sigma} = p_h \frac{\partial G}{\partial p_h} + p_z \frac{\partial G}{\partial p_z} \qquad (4)$$

Since we assume $f = \text{const}$, the vertical time derivative in equation 3 comprises three terms,

$$\frac{\partial G}{\partial t_o} = \frac{\partial G}{\partial V}\cdot\frac{dV}{dt_o} + \frac{\partial G}{\partial \delta}\cdot\frac{d\delta}{dt_o} + \frac{\partial G}{\partial \varepsilon}\cdot\frac{d\varepsilon}{dt_o} \qquad (5)$$

Finally, we replace the second equation of set 3 by

$$\frac{dt_o}{d\sigma} = \frac{dt_o}{dz} \cdot \frac{dz}{d\sigma} = \frac{\partial G / \partial p_z}{V} \qquad (6)$$

Boundary Value Ray Tracing

The curved ray path is presented in Figure 1. Points S and R are source and receiver locations on the earth surface, I the image point, U is the projection of the image point on the earth surface, and N is the intersection of the normal line to the reflection surface (that passes through the image point I) with the earth surface. Note that the length (offset) and the direction (azimuth) of vector $\overrightarrow{SR}$ are specified and not the specific locations of S and R.

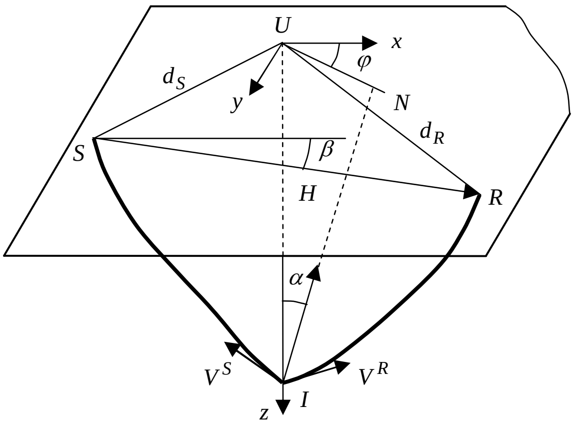

Figure 1. Boundary value ray tracing

In case of a tilted normal to the reflection surface, the planes of incident and reflected paths are different. The curved path IS of the incident ray is in the vertical plane ISU, and that of the reflected ray is in another vertical plane IRU. Azimuths of these two vertical planes are different. At the reflection point I, the incident ray velocity V^S, the reflected ray velocity V^R and the normal IN to the reflection surface are in the same (non-vertical) plane SIR. The inward normal IN to the reflection surface is defined by the dip angle α and azimuth φ. The source-receiver offset SR in the horizontal plane is described by its absolute value H and azimuth β. Let d_S and d_R be lateral shifts of the incident and the reflected ray, respectively. They depend on the corresponding horizontal slowness p_h^R and p_h^S. These shifts result from the initial value ray tracing,

$$\begin{aligned} d_R\left(p_h^R\right) \cdot \cos\varphi^R - d_S\left(p_h^S\right) \cdot \cos\varphi^S &= H\cos\beta \\ d_R\left(p_h^R\right) \cdot \sin\varphi^R - d_S\left(p_h^S\right) \cdot \sin\varphi^S &= H\sin\beta \end{aligned} \quad , \qquad (7)$$

where φ^S and φ^R are azimuth angles of shifts d_S and d_R, respectively. Let vector $\vec{n}$ be a normal to the reflection surface. For a general anisotropic medium, the Snell's reflection law is

$$\left(\vec{p}^S + \vec{p}^R\right) \times \vec{n} = 0 \quad . \qquad (8)$$

Vector equation 8 is equivalent to three scalar equations, but only two of them are linearly independent. Thus, we have four equations (7 and 8) to establish the horizontal slowness and the azimuth angles of the incident and the reflected ray.

Residual Traveltime

Perturbations of the VTI properties affect the residual traveltime. The perturbed parameters of the medium are vertical velocity V and two Thomsen parameters, ε and δ. Perturbations are assumed small, and the response of the medium is linearized. It follows from equation 6 that the residual traveltime along the ray is

$$\Delta t = \sum_{k=1}^{N} \int_{\sigma_k} \left(\Delta p_h \cdot \frac{\partial G}{\partial p_h} + \Delta p_z \cdot \frac{\partial G}{\partial p_z} \right) d\sigma \qquad (9)$$

where k is the layer index. The Hamiltonian vanishes along the ray, and its variation is identically zero. The one-way residual traveltime equation becomes

$$\Delta t = -\sum_{k=1}^{N} \int_{\sigma_k} \left(\frac{\partial G}{\partial V} \Delta V_k + \frac{\partial G}{\partial \varepsilon} \Delta\varepsilon_k + \frac{\partial G}{\partial \delta} \Delta\delta_k \right) d\sigma \qquad (10)$$

Shift of Reflection Point in Depth

There are two factors that cause variation of traveltime: residuals of medium properties and shift of the reflection point in depth (Koren *et al.*, 1999). We assume that the zero offset traveltime is preserved. The medium properties change, and therefore the depth of the reflection point varies accordingly. Let $\Delta t_{\mathrm{m}}^{\mathrm{zo}}$ be the one-way zero offset traveltime change caused by the medium properties variation only. It can be established by equation 11 applied for the zero offset ray. Let Δz be the change of depth of the reflection point. The variation of traveltime Δt_{d} caused solely by this vertical shift is

$$\Delta t_{\mathrm{d}} = \Delta t_{\mathrm{d}}^S + \Delta t_{\mathrm{d}}^R = \Delta z \cdot \Delta P_z \qquad (11)$$

where ΔP_z is the change of vertical "ray slowness",

$$\Delta P_z = \frac{\cos\alpha_{\mathrm{ray}}^S}{V_{\mathrm{ray}}^S} + \frac{\cos\alpha_{\mathrm{ray}}^R}{V_{\mathrm{ray}}^R} \quad . \qquad (12)$$

Conservation of the two-way zero offset traveltime reads

$$\Delta t_{\mathrm{d}}^{\mathrm{zo}} = -2\Delta t_{\mathrm{m}}^{\mathrm{zo}} \quad . \qquad (13)$$

This yields an explicit expression for variation of depth,

$$\Delta z = \frac{2}{\Delta P_{\mathrm{z}}^{\mathrm{zo}}} \sum_{k=1}^{N} \int_{\sigma_k} \underbrace{\left(\frac{\partial G}{\partial V_P}\Delta V_k + \frac{\partial G}{\partial \varepsilon}\Delta \varepsilon_k + \frac{\partial G}{\partial \delta}\Delta \delta_k \right)}_{\text{zero offset}} d\sigma \qquad (14)$$

where $\Delta P_{\mathrm{z}}^{\mathrm{zo}}$ is defined in equation 12, for the zero offset ray. A similar characteristic $\Delta P_{\mathrm{z}}^{i}$ can de defined for any given nonzero offset. Variation of depth Δz is the same for all offsets. However, the change in traveltime, caused by this variation, is different for different offsets i,

$$\Delta t_{\mathrm{d}}^{i} = 2\frac{\Delta P_{\mathrm{z}}^{i}}{\Delta P_{\mathrm{z}}^{\mathrm{zo}}} \sum_{k=1}^{N} \int_{\sigma_k} \underbrace{\left(\frac{\partial G}{\partial V}\Delta V_k + \frac{\partial G}{\partial \delta}\Delta \delta_k + \frac{\partial G}{\partial \varepsilon}\Delta \varepsilon_k \right)}_{\text{zero offset}} d\sigma \qquad (15)$$

Tomographic Coefficients

Introduce the tomographic coefficients

$$A_k^m = -\underbrace{\int_{\sigma_k} \frac{\partial G}{\partial m} d\sigma}_{\text{incident, offset } i} - \underbrace{\int_{\sigma_k} \frac{\partial G}{\partial m} d\sigma}_{\text{reflected, offset } i} + 2\frac{\Delta P_{\mathrm{z}}^{i}}{\Delta P_{\mathrm{z}}^{\mathrm{zo}}} \cdot \underbrace{\int_{\sigma_k} \frac{\partial G}{\partial m} d\sigma}_{\text{zero offset}}$$

$$\text{where} \quad m = \{V, \delta, \varepsilon\} \quad \text{and} \quad A_k^m = \left\{ A_k^V, A_k^\delta, A_k^\varepsilon \right\} \qquad (16)$$

After ray tracing is done, A_k^V, A_k^ε, A_k^δ are known values along the rays. The two-way residual traveltime reads

$$\Delta t = \sum_{k=1}^{N} A_k^V \Delta V_k + A_k^\varepsilon \Delta \varepsilon_k + A_k^\delta \Delta \delta_k \quad . \qquad (17)$$

Equations 16 and 17 express the linearized relation between the model parameter perturbations and residual traveltime.

Local Approach: Single Parameter Scanning

Local tomography is a layer stripping approach performed for single locations and for a single parameter type m. This approach is an interactive "coherency inversion" analysis type which is performed directly along the migrated image gathers (Koren *et al.*, 1999). It is recommended to first select some sparse locations along the layer where the residual moveouts are sensitive to the model changes. Then the analysis can be performed in a batch mode for the whole layer, scanning residual model parameters within a specified range. The output is a horizon-based semblance plot for a layer, where the maximum amplitudes indicate the considered model perturbations**.** The resolving equations are 16 and 17, and each time only one of the residuals $\{\Delta V_k, \Delta\delta_k, \Delta\varepsilon_k\}$ is scanned. The interval velocities (or alternatively δ) are updated using the short-offset reflection events ($\le 30^o$), while ε is updated using the long-offset data. Steep dips in the model contribute considerably to the sensitivity of the residual moveouts to changes in parameter ε. This approach suffers from general limitations of layer stripping methods: the inaccuracies of the parameter estimation in the overburden affect the parameters of the current layer.

Figures 2 and 3 demonstrate a simple synthetic example. The vertical profile of the true VTI parameters: interval velocity, δ and ε, with the corresponding synthetic gather (calculated by anisotropy ray tracing) are shown in Figure 2. In this example, the velocity and δ are considered known and exact, and the goal is to update ε.

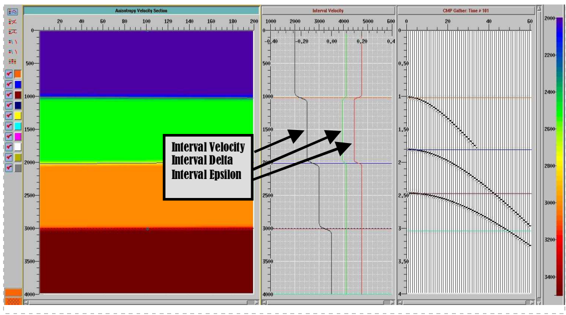

Figure 2. Synthetic anisotropy model

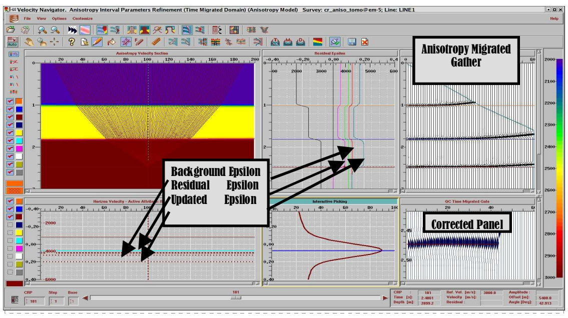

Figure 3. Epsilon correction at the third layer: true 0.2, background 0.125, residual 0.06

We set the initial guess $\varepsilon = \delta$ at all layers. Anisotropy curved ray time migration was performed. The non-flatten gathers are shown in the right part of Figure 3. The figure shows the ε analysis in the third layer. The first and second layers have already been inverted. The corresponding ε updates are shown in the vertical and the horizon Velocity Panels. An ε histogram is performed, where the optimal residual corresponds to the maximum coherency value. The corresponding flatten event is shown in the Corrected Panel display. The residual ε values for the three layers are underestimated (e.g., for the third layer, the updated $\varepsilon = 0.185$ as compared to the true value 0.2). Another iteration was applied with the corrected values which resulted in almost perfect values.

Global Approach

Global tomography for residual parameter update is intensively used in depth imaging (Farra and Madariaga, 1988; Stork, 1992; Kosloff *et al.*, 1996, among others). In this section we describe a global inversion procedure for a locally varying anisotropy 1D model (time-migrated domain). The results of the local tomographic inversion are used as a background model for the global tomography. The global inversion yields all residuals simultaneously, for a fixed lateral location. The reflecting image points (elements) are stored as a set of vertical *pencils*. Each *pencil* is a vertical function, containing information about the local reflecting surfaces intersection points with the local vertical time axis. Each intersection point contains information about its vertical time value, local surface's normal vector (dip and azimuth angles) and the formation index above it. In addition, at each point (node) we store the traveltime errors (residual time moveouts) related to the reflected image point. The residual times are functions of offsets or reflection angles with a given shot receiver orientation (azimuth) along the earth surface (in marine data, the azimuth is the shooting direction). Lateral location of pencils may be sparse and irregular. Vertical nodes may also be irregular and different for different pencils. Within each output interval, the residual parameters Δm are considered constant. The upper and lower interfaces of the intervals do not necessarily coincide with the pencil nodes. The dimensionality of the problem depends on the amount of the output intervals N^{out} and is independent on the amount of the pencil nodes N. Since the problem is over-determined, the least-squares approach is used. The resolving matrix M consists of $N^{\text{out}} \times N^{\text{out}}$ blocks, where each block has a dimension of 3×3 (three parameters Δm). The right-side vector B consists of N^{out} blocks, each of length 3. The structure of the blocks is

$$M_{k_r,k_c}^{m_r,m_c} = \sum_{n=0}^{N-1}\sum_{i=0}^{N_n^h-1} \frac{A_{n,i,k_r}^{m_r} \cdot A_{n,i,k_c}^{m_c}}{N_n^h \cdot S_{n,i}^{\text{data}}} + \frac{N}{3N^{\text{out}}} \cdot \frac{\delta_{k_r,k_c}^{k} \cdot \delta_{m_r,m_c}^{k}}{S_{k_r}^{m_r}}$$

$$B_{k_r}^{m_r} = \sum_{n=0}^{N-1}\sum_{i=0}^{N_n^h-1} \frac{A_{n,i,k_r}^{m_r} \cdot \Delta t_{n,i}}{N_n^h \cdot S_{n,i}^{\text{data}}} \qquad (18)$$

where N_n^h is the amount of offsets for pencil node n, $0 \le k_r \le N^{\text{out}} - 1$ and $0 \le k_c \le N^{\text{out}} - 1$ are row index and column index, respectively, of a block in the global matrix or vector. Superscripts $0 \le m_r \le 2$ and $0 \le m_c \le 2$ specify the medium property. Factor $A_{n,i,k_r}^{m_r}$ is the tomographic coefficient of medium property m_r obtained from a ray with offset index i and reflection point n within the output interval k_r. Data variance $S_{n,i}^{\text{data}}$ is related to reliability of traveltime residual for reflection point n and offset i (usually all offsets have the same reliability). Model variance $S_{k_r}^{m_r}$ is related to property m_r on the output interval k_r, and δ^k is the Kronecker symbol. The standard deviation of the model parameter is assumed proportional to the interval thickness. Within the thin output interval, the information is insufficient, and thus the variation of the medium properties on this interval with respect to the background model should be limited.

Conclusions

We have described two complementary tomographic approaches for VTI parameter determination. The local tomography enables a controlled interactive estimation of the long-wavelength anisotropy parameters. In the global approach we invert simultaneously for all parameters of all output intervals using detailed residual moveout information. The reliable anisotropy parameters estimated by the local approach are used as a background (guiding) model for the global one. This makes it possible to further apply successfully the global constrained least-squares approach.

Acknowledgement

We wish to thank Vladimir Grechka for numerous helpful discussions on the range of anisotropic parameters.

References

Farra V., and R. Madariaga, 1988, Nonlinear reflection tomography: Geophysical Journal International, **95**, 135-147.

Koren, Z., U. Zackhem, and D. Kosloff, 1999, 3D local tomography – residual interval velocity analysis on a depth solid model: 69th Annual International Meeting, SEG, Expanded Abstracts, 1255-1258.

Stork, C., 1992, Reflection tomography for the post-migrated domain: Geophysics, **57**, 680-692.

Thomsen, L., 1986, Weak elastic anisotropy: Geophysics, **51**, 1954-1966.

Tsvankin, I., 2001, Seismic signatures and analysis of reflection data in anisotropic media: Elsevier Science Ltd.

EDITED REFERENCES

Note: This reference list is a copy-edited version of the reference list submitted by the author. Reference lists for the 2006 SEG Technical Program Expanded Abstracts have been copy edited so that references provided with the online metadata for each paper will achieve a high degree of linking to cited sources that appear on the Web.

REFERENCES

Farra V., and R. Madariaga, 1988, Nonlinear reflection tomography: Geophysical Journal International, **95**, 135–147.

Koren, Z., U. Zackhem, and D. Kosloff, 1999, 3D local tomography – residual interval velocity analysis on a depth solid model: 69th Annual International Meeting, SEG, Expanded Abstracts, 1255–1258.

Stork, C., 1992, Reflection tomography for the postmigrated domain: Geophysics, **57**, 680–692.

Thomsen, L., 1986, Weak elastic anisotropy: Geophysics, **51**, 1954–1966.

Tsvankin, I., 2001, Seismic signatures and analysis of reflection data in anisotropic media: Elsevier Science Publisging Company, Inc.